



Pergamon

Available online at www.sciencedirect.com

SCIENCE @ DIRECT®



Acta Materialia 51 (2003) 1271–1281

www.actamat-journals.com

Spatial correlations and higher-order gradient terms in a continuum description of dislocation dynamics

I. Groma^{a,*}, F.F. Csikor^a, M. Zaiser^b

^a Department of General Physics, Eötvös University, PO BOX 32,1518 Budapest, Hungary

^b Centre for Materials Science and Engineering, University of Edinburgh, King's Buildings, Sanderson Building, Edinburgh EH9 3JL, UK

Received 6 August 2002; accepted 23 October 2002

Abstract

The problem of the collective behavior of straight parallel edge dislocations is investigated. Starting from the equation of motion of individual dislocations a continuum description is derived. It is shown that the influence of the short range dislocation-dislocation interactions on the dislocation dynamics can be well described by a local back stress which scales like the square root of dislocation density plus a non-local diffusion-like term. The value of the corresponding diffusion coefficient is determined numerically, and implications for size effects in plasticity are discussed.

© 2003 Acta Materialia Inc. Published by Elsevier Science Ltd. All rights reserved.

Keywords: Dislocations; Theory and modeling of defects; Mechanical properties

1. Introduction

A main goal in the theory of crystal plasticity is the derivation of continuum constitutive relations from the underlying dynamics of systems of discrete dislocations. One approach to achieve this goal is to perform the discrete-to continuum transition on the dislocation dynamics level, adopting a formulation of dislocation dynamics in terms of appropriately defined dislocation densities.

Several attempts have been made towards a continuum description of dislocation dynamics which

accounts for the collective behavior of the dislocations. In the models of Holt [1] and Ricman & Vifials [2], an irreversible thermodynamics analogy was used, Walgraef and Aifantis elaborated an approach where different dislocation populations evolve according to reaction-diffusion equations [3–5], Kratochvil et al. developed the idea of non-local hardening based on particular mechanisms such as dislocation sweeping [6,7] and Hähner and Zaiser proposed a stochastic description of dislocation dynamics in terms of nonlinear stochastic processes [8,9]. Most of these models are based on analogies with other physical problems like spinodal decomposition, oscillating chemical reactions and chemical patterning, etc. As a consequence of this, the properties of individual dislocations are taken into account only in a very indirect way. In

* Corresponding author. Tel.: +36-1372-2802; fax: +36-1372-2811.

E-mail address: groma@metal.elte.hu (I. Groma).

most of these models the collective nature of dislocation motion is described by diffusion-like gradient terms. Since the balance equations are quite heuristic, the actual values of diffusion coefficients are difficult to estimate, the meaning of the associated internal length scales is often unclear, and one may even ask whether it is possible at all to describe dislocation interactions in gradient terms. Hence, the question arises whether it is possible to devise more rigorous procedures to obtain a continuum description of dislocation dynamics from the dynamics of discrete dislocations.

It has been shown by Groma et al. [10,11] that for a system of straight parallel dislocations a continuum description can be rigorously derived from the equations of motion of individual dislocations. Using a different approach, a continuum description of the dynamics of a system of curved dislocations in three dimensions was formulated by El-Azab [12]. However, a major drawback of these earlier investigations is that in order to get a closed set of equations short range dislocation-dislocation correlations have been neglected and dislocation-dislocation interactions were described only by the long-range term which is the self-consistent stress field.

The general properties of dislocation-dislocation correlation functions were investigated in detail in [13]. The goal of the present paper is to demonstrate that the influence of short range dislocation-dislocation correlations can be taken into account by a local flow stress which scales like the square root of dislocation density, plus a gradient term. The value of the corresponding ‘diffusion’ coefficient is determined. For illustration we demonstrate on a simple example how this description term leads to size effects in a constrained thin layer.

2. Linking discrete and continuum dislocation dynamics descriptions

Let us consider N straight parallel edge dislocations with positions $\{\vec{r}_i, i = 1..N\}$ in the plane perpendicular to the line vector \vec{l} . For the sake of simplicity we envisage a single-glide configuration, i.e., the Burgers vector of the i th dislocation can

have only the values $\vec{b}_i = \pm \vec{b}$. Assuming overdamped dislocation motion, the velocity of the i th dislocation is given by

$$\vec{v}_i = B\vec{b} \left(\sum_{j \neq i}^N s_j s_i \tau_{\text{ind}}(\vec{r}_i - \vec{r}_j) + s_i \tau_{\text{ext}} \right) \quad (1)$$

where $s_i = \vec{b}_i / \vec{b}$ (\vec{b}^2) is the sign of the dislocation, $\tau_{\text{ind}}(\vec{r}_i - \vec{r}_j)$ is the shear stress created at \vec{r}_i by a positive dislocation located at \vec{r}_j , τ_{ext} is the external stress, and B is the dislocation mobility. In the following we drop the constant B which can always be absorbed into the time variable.

The discrete dislocation system of Eq. (1) can be formally characterized by discrete densities of positive and negative dislocations, $\rho_+^D(\vec{r}) = \sum_{j, s_j = 1} \delta(\vec{r} - \vec{r}_j)$ and $\rho_-^D(\vec{r}) = \sum_{k, s_k = -1} \delta(\vec{r} - \vec{r}_k)$. To arrive at a continuum description, we average over an ensemble of statistically equivalent dislocation systems (for details of the averaging procedure see [10,11]). From Eq. (1) we obtain the following balance equations for the time evolution of the ensemble averaged dislocation densities $\rho_+ = \langle \rho_+^D \rangle$ and $\rho_- = \langle \rho_-^D \rangle$:

$$\begin{aligned} \frac{\partial \rho_+(\vec{r}_1, t)}{\partial t} + \vec{b} \frac{\partial}{\partial \vec{r}_1} \left[\rho_+(\vec{r}_1, t) \tau_{\text{ext}} \right. \\ \left. + \int \{ \rho_{++}(\vec{r}_1, \vec{r}_2, t) - \rho_{+-}(\vec{r}_1, \vec{r}_2, t) \} \tau_{\text{ind}}(\vec{r}_1 \right. \\ \left. - \vec{r}_2) d\vec{r}_2 = 0 \right] \end{aligned} \quad (2)$$

$$\begin{aligned} \frac{\partial \rho_-(\vec{r}_1, t)}{\partial t} + \vec{b} \frac{\partial}{\partial \vec{r}_1} \left[-\rho_-(\vec{r}_1, t) \tau_{\text{ext}} \right. \\ \left. + \int \{ \rho_{--}(\vec{r}_1, \vec{r}_2, t) - \rho_{-+}(\vec{r}_1, \vec{r}_2, t) \} \tau_{\text{ind}}(\vec{r}_1 - \vec{r}_2) d\vec{r}_2 = 0 \right] \end{aligned} \quad (3)$$

Here the operator $[\partial / \partial \vec{r}_1]$ denotes the divergence with respect to the coordinate vector \vec{r}_1 . The two-particle density functions appearing in the integrals may be interpreted as follows: $\rho_{++}(\vec{r}_1, \vec{r}_2, t) dV_1 dV_2$ is the joint probability to find at time t a positive dislocation in a volume element dV_1 at \vec{r}_1 and another positive dislocation in a volume element dV_2 at \vec{r}_2 . The two-particle density functions ρ_{+-} and ρ_{-+} are ρ_{--} interpreted accordingly. The negative signs in front of ρ_{+-} and

ρ_{-+} in Eqs. (2) and (3) come from the simple fact that the interaction force between dislocations of equal signs has the opposite direction as that between dislocations of different signs.

By adding and subtracting the above two equations, the following evolution equations can be obtained for the total dislocation density $\rho(\vec{r}, t) = \rho_+(\vec{r}, t) + \rho_-(\vec{r}, t)$ and for the sign dislocation density $\kappa(\vec{r}, t) = \rho_+(\vec{r}, t) - \rho_-(\vec{r}, t)$:

$$\begin{aligned} \frac{\partial \rho(\vec{r}_1, t)}{\partial t} + \vec{b} \frac{\partial}{\partial \vec{r}_1} [\kappa(\vec{r}_1, t) \tau_{ext} + \int \{ \rho_{++}(\vec{r}_1, \vec{r}_2, t) \\ + \rho_{--}(\vec{r}_1, \vec{r}_2, t) - \rho_{+-}(\vec{r}_1, \vec{r}_2, t) \\ - \rho_{-+}(\vec{r}_1, \vec{r}_2, t) \} \tau_{ind}(\vec{r}_1 - \vec{r}_2) d\vec{r}_2] = 0 \end{aligned} \quad (4)$$

$$\begin{aligned} \frac{\partial \kappa(\vec{r}_1, t)}{\partial t} + \vec{b} \frac{\partial}{\partial \vec{r}_1} [\rho(\vec{r}_1, t) \tau_{ext} + \int \{ \rho_{++}(\vec{r}_1, \vec{r}_2, t) \\ + \rho_{--}(\vec{r}_1, \vec{r}_2, t) - \rho_{+-}(\vec{r}_1, \vec{r}_2, t) \\ + \rho_{-+}(\vec{r}_1, \vec{r}_2, t) \} \tau_{ind}(\vec{r}_1 - \vec{r}_2) d\vec{r}_2] = 0 \end{aligned} \quad (5)$$

The connection with plasticity theory is established by considering the ensemble-averaged shear strain rate $\dot{\gamma}(\vec{r}, t) = \vec{b} \langle \rho_+^D \vec{v}_+(\vec{r}, t) = \rho_-^D \vec{v}_-(\vec{r}, t) \rangle$. It turns out that this fulfill the relation (cf. e.g. [14])

$$\frac{\partial \kappa}{\partial t} = - \frac{\vec{b} \partial \dot{\gamma}}{b^2 \partial \vec{r}}, \quad (6)$$

i.e., the sign dislocation density κ is related to the gradient of the shear strain γ by $\kappa = \vec{b}(\partial \gamma / \partial \vec{r}) / b^2$. Hence, κ , corresponds to the “geometrically necessary” dislocation density.

It is important to note that Eqs. (4) and (5) are exact, i.e. no assumption is required to derive them from Eq. (1). Since, however, they depend on the two-particle density functions they do not form a closed set of equations. Although equations can be derived for the two-particle densities, these depend on the three-particle densities and so on, resulting in an infinite hierarchy of equations [10,13]. In order to get usable results this hierarchy has to be cut by assuming that density functions of a certain order can be built up from the lower order ones.

The simplest possible assumption is that the two-particle densities are products of the single-particle ones, i.e. $\rho_{ss'}(\vec{r}_1, \vec{r}_2, t) = \rho_s(\vec{r}_1) \rho_{s'}(\vec{r}_2)$, $s, s' \in \{+, -\}$.

As explained in detail in [10] this leads to a self-consistent type of dislocation dynamics described by the equations

$$\frac{\partial \rho(\vec{r}, t)}{\partial t} + \vec{b} \frac{\partial}{\partial \vec{r}} [\kappa(\vec{r}, t) \{ \tau_{sc}(\vec{r}, t) + \tau_{ext} \}] = 0, \quad (7)$$

$$\frac{\partial \kappa(\vec{r}, t)}{\partial t} + \vec{b} \frac{\partial}{\partial \vec{r}} [\rho(\vec{r}, t) \{ \tau_{sc}(\vec{r}, t) + \tau_{ext} \}] = 0, \quad (8)$$

where

$$\tau_{sc}(\vec{r}) = \int \kappa(\vec{r}_1, t) \tau_{ind}(\vec{r} - \vec{r}_1) d\vec{r}_1 \quad (9)$$

is a self-consistent internal-stress field.

It needs to be mentioned that dislocation annihilation and/or multiplication can be incorporated into this framework. This leads to additional source terms on the right-hand side of Eq. (7). However, Eq. (8) remains unchanged, reflecting the fact that the net Burgers vector of the system is conserved.

3. Pair correlations and diffusion terms in the dislocation dynamics

The self-consistent field approximation discussed in the previous section neglects short-range dislocation-dislocation correlations, i.e., it corresponds to the assumption that the dislocation arrangement is microscopically random. On the other hand it is known that non-vanishing correlations are essential to understanding the energetics of dislocation systems [15], the statistics of internal stresses [16], the properties of X-ray line profiles [17], and the short-range interactions between dislocations [13]. Most importantly, it has been demonstrated that dislocation-dislocation correlations may introduce an internal length scale into the dislocation dynamics and into associated plasticity theories [13,18,19]. One possibility to take into account short range correlation effects is to assume that $\rho_{ss'}(\vec{r}_1, \vec{r}_2, t)$ is given in the form

$$\rho_{ss'}(\vec{r}_1, \vec{r}_2, t) = \rho_s(\vec{r}_1) \rho_{s'}(\vec{r}_2) (1 + d_{ss'}(\vec{r}_1 - \vec{r}_2)) \quad s, s' \in \{+, -\} \quad (10)$$

where $d_{ss'}$, corresponds to the correlation function in a homogeneous dislocation system. As a conse-

quence of this, d_{ss} depends only on the relative coordinate $\vec{r}_1 - \vec{r}_2$. Using the expression (10), Eqs. (4, 5) may be written as

$$\frac{\partial \rho(\vec{r}, t)}{\partial t} + \vec{b} \frac{\partial}{\partial \vec{r}} [\kappa(\vec{r}, t) \{ \tau_{sc}(\vec{r}) + \tau_{ext} - \tau_f(\vec{r}) + \tau_b(\vec{r}) \}] = 0, \quad (11)$$

$$\frac{\partial \kappa(\vec{r}, t)}{\partial t} + \vec{b} \frac{\partial}{\partial \vec{r}} [\rho(\vec{r}, t) \{ \tau_{sc}(\vec{r}) + \tau_{ext} - \tau_f(\vec{r}) + \tau_b(\vec{r}) \}] = 0, \quad (12)$$

where

$$\tau_f(\vec{r}) = \frac{1}{2} \int \rho(\vec{r}_1) d^a(\vec{r} - \vec{r}_1) \tau_{ind}(\vec{r} - \vec{r}_1) d\vec{r}_1, \quad (13)$$

$$\tau_b(\vec{r}) = \int \kappa(\vec{r}_1) d(\vec{r} - \vec{r}_1) \tau_{ind}(\vec{r} - \vec{r}_1) d\vec{r}_1. \quad (14)$$

Here $d^a(\vec{r}) = 1/2[d_{+-}(\vec{r}) - d_{-+}(\vec{r})]$ and $d(\vec{r}) = 1/4[d_{++}(\vec{r}) + d_{--}(\vec{r}) + d_{+-}(\vec{r}) + d_{-+}(\vec{r})]$. The details of the derivation of these relations are given in the Appendix.

The actual form of the functions $d(\vec{r})$ and $d^a(\vec{r})$ can be determined from discrete dislocation dynamics simulations (for details see [13]). For better statistics simulations need to be performed for several different (but statistically equivalent) initial configurations. A result is shown in Fig. 1. Here the pair correlation function $d(\vec{r})$ has been determined from 100 simulations of systems of 2048 positive and 2048 negative dislocations after relaxation of the dislocation arrangement from an initially random configuration at zero external stress. Because of the general scaling properties of dislocation-dislocation correlation functions, simulations of systems with different densities yield the same result when the space coordinate is scaled by the dislocation spacing, i.e., d depends only on the scaled coordinate $\vec{r}/\sqrt{\rho}$ [13]. Fig. 1 can be interpreted as follows. For a dislocation located in the origin, the function $d(\vec{r})$ gives the probability to find correlated partners at $d\vec{r}$, irrespective of the signs of both dislocations. We observe positive correlations under 45 degrees (dipoles of dislocations of opposite signs) as well as in the 90 degree orientations (walls of dislocations of the same sign), and there is a short-range anticorrel-

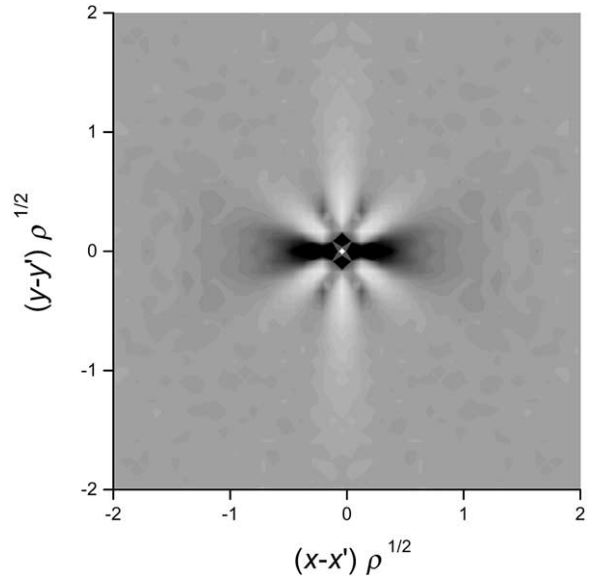


Fig. 1. Pair correlation function $d(\vec{r})$ of a dislocation system as discussed in the text, after relaxation at zero external stress. The x and y coordinates have been scaled by the mean dislocation spacing $1/\sqrt{\rho}$. Light areas correspond to positive pair correlations, dark areas to negative correlation.

ation in the 0 and 180 degree orientations (pile-up configurations).

One observes that the dislocation-dislocation correlation functions decay to zero within a few dislocation distances. Because of this in the integrals in Eqs. (13, 14) the functions $\kappa(\vec{r}_1)$ and $\rho(\vec{r}_1)$ can be approximated by their Taylor expansion around the point \vec{r} . Keeping only the first non-vanishing terms we arrive at

$$\tau_f(\vec{r}) = \frac{\rho(\vec{r})}{2} \int d^a(\vec{r}) \tau_{ind}(\vec{r}) d\vec{r}, \quad (15)$$

$$\tau_b(\vec{r}) = -\frac{\partial \kappa(\vec{r})}{\partial \vec{r}} \int r d(\vec{r}) \tau_{ind}(\vec{r}) d\vec{r}. \quad (16)$$

We now use that $d(\vec{r})$ and $d^a(\vec{r})$ are functions of $\sqrt{\rho}\vec{r}$ only, and that the shear stress $\tau_{ind}(\vec{r})$ is proportional to $1/r$. Hence we may rewrite Eq. (15) as

$$\tau_f(\vec{r}) = \frac{\sqrt{\rho(\vec{r})}}{2} \int d^a(\vec{x}) \tau_{ind}(\vec{x}) d^2\vec{x}, \quad \vec{x} = \sqrt{\rho}\vec{r}. \quad (17)$$

Using the symmetry properties of $d^a(\vec{r})$ (it is an

odd function) and inserting the actual form $\tau_{\text{ind}}(\vec{r})$ this can be simplified to

$$\tau_f(\vec{r}) = \frac{AC}{2} b \sqrt{\rho(\vec{r})} \quad (18)$$

where $A = \mu/[2\pi(1 - \nu)]$, μ is the shear modulus, ν is the Poisson ratio, and

$$C = \int \frac{x(x^2 - y^2)}{(x^2 + y^2)^2} d^a(x, y) dx dy \quad (19)$$

The stress contribution τ_f is related to the correlation function d^a which in physical terms characterizes the polarization of dipoles of dislocations of opposite signs. If the acting stress (the sum of all other stress contributions in Eqs. (11) and (12)) is small, the system evolves towards a ‘jammed phase’ where τ_f offsets the acting stress. However, τ_f can increase only up to a certain value where dipoles and multipoles break up. This value, where the dislocation system undergoes a transition to a ‘moving phase’ as discussed by Miguel et al. [20], can be interpreted as the local flow stress. From Eq. (18) it follows that this stress scales like the square root of dislocation density, which is indeed satisfactory.

We now turn to the gradient-dependent stress contribution τ_b . Repeating the above procedure we find that

$$\tau_b(\vec{r}) = -\frac{\partial \kappa(\vec{r})}{\partial \vec{r}} \frac{1}{\rho(\vec{r})} \int \vec{x} d(\vec{x}) \tau_{\text{ind}}(\vec{x}) d^2 \vec{x}. \quad (20)$$

From this it follows that

$$\tau_b(\vec{r}) = -\frac{AD\vec{b}\partial\kappa(\vec{r})}{\rho \partial\vec{r}} \quad (21)$$

where

$$D = \int \frac{x^2(x^2 - y^2)}{(x^2 + y^2)^2} d(x, y) dx dy \quad (22)$$

is a non-dimensional constant. We note that because of Eq. (6), the stress contribution τ_b depends on the second derivative of the strain, $\tau_b = -[D/\rho]\partial^2\gamma/\partial x^2$ where x denotes the spatial coordinate in the direction of slip. Hence, τ_b can be envisaged as a second-order gradient contribution to the flow stress as postulated by Aifantis

[21]. The corresponding gradient coefficient is inversely proportional to the dislocation density, i.e., the length scale associated with the gradient term is proportional to the dislocation spacing.

To evaluate the constant D , it is useful to revert to polar coordinates (r, ϕ) where $r = \sqrt{x^2 + y^2}$ and $\phi = \arctan(y/x)$. Since the term in front of d in Eq. (22) depends only on the angle, by integrating over the radial direction we find that

$$D = \int \cos^2\phi(\cos^2\phi - \sin^2\phi) d_{\text{ang}}(\phi) d\phi \quad (23)$$

where the angular correlation $d_{\text{ang}}(\phi) = \int d(r, \phi) dr$ is the integral of the pair correlation function over the radial direction. Physically this function gives the probability to find a pair of dislocations under the angle ϕ irrespective of distance and sign, minus the respective probability in an entirely random configuration. Fig. 2 shows the function $d_{\text{ang}}(\phi) = d_{\text{ang}}^0$ for a dislocation arrangement emerging after relaxation of an initially random dislocation pattern, i.e., the situation depicted in Fig. 1. It is seen that we observe four peaks in the 0, 45, and 90 degree orientations. While the peaks in the 45 and 90 degree orientations are evident from Fig. 1, the peak in the 0 degree pile-up orientation requires some explanation. This peak arises from the fact that dislocations of the same sign close to that orientation repel each other, which tends to align them under 0 (or 180) degrees. However, this alignment is visible only after radial averaging

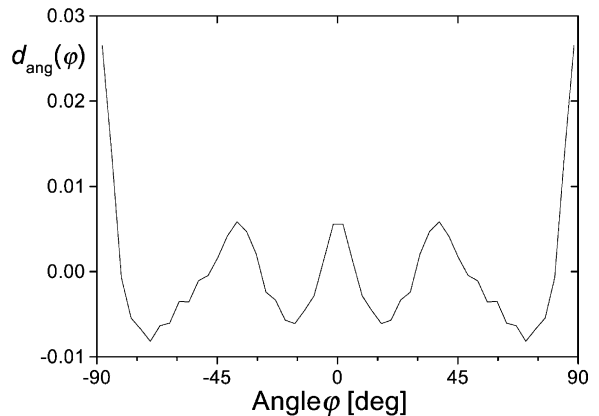


Fig. 2. Angular correlation function $d_{\text{ang}}^0(\phi)$ for the same system as in Fig. 1, after [20].

since, on short distances, one actually gets an anti-correlation as seen from Fig. 1.

Computing D from the correlation function d_{ang}^0 in Fig. 2, yields $D_0 \approx 0$. However, the picture changes if one takes into account that dislocations are emitted by sources, i.e., they are created in geminate pairs on the same slip plane. Denoting the number of dislocation pairs that are emitted from a source by N_p , and assuming that the sources are distributed at random, one finds that the actual angular correlation function can be written approximately as

$$d_{\text{ang}}(\phi) \approx d_{\text{ang}}^0(\phi) + [(N_p - 1)/2][\delta(\phi) + \delta(\phi - \pi) - 1/\pi] \quad (24)$$

where δ is the delta function. Evaluating D with this function yields

$$D \approx 3(N_p - 1)/4 \quad (25)$$

i.e., D is proportional to the average number of geminate partners of a dislocation that stem from the same source. This expression remains valid even if dislocations may annihilate, leading to a loss of correlated partners; N_p in this case has to be interpreted as the average number of surviving partners that remain in the system.

After substituting the expression (21) into Eqs. (11, 12) and defining the effective stress $\tau_{\text{eff}} = \tau_{\text{ext}} - \tau_f$, we find the following constitutive equations:

$$\frac{\partial \rho(\vec{r}, t)}{\partial t} + \vec{b} \frac{\partial}{\partial \vec{r}} \left[\kappa(\vec{r}, t) \left\{ \tau_{\text{sc}}(\vec{r}, t) + \tau_{\text{eff}} - AD \frac{\vec{b}}{\rho(\vec{r}, t)} \frac{\partial \kappa(\vec{r}, t)}{\partial \vec{r}} \right\} \right] = 0 \quad (26)$$

$$\frac{\partial \kappa(\vec{r}, t)}{\partial t} + \vec{b} \frac{\partial}{\partial \vec{r}} \left[\rho(\vec{r}, t) \left\{ \tau_{\text{sc}}(\vec{r}, t) + \tau_{\text{eff}} - AD \frac{\vec{b}}{\rho(\vec{r}, t)} \frac{\partial \kappa(\vec{r}, t)}{\partial \vec{r}} \right\} \right] = 0 \quad (27)$$

These equations account for both the long-range (in terms of the self-consistent stress τ_{sc}) and the short-range dislocation interactions (in terms of a reduced effective stress and the gradient-dependent stress contribution). In the next section we will demonstrate how these relations can be used to

evaluate size effects in a simple system, namely a constrained channel deforming in simple shear.

4. Deformation of a constrained channel

To illustrate some implications of the constitutive equations derived in the previous section we study a most simple example, namely a constrained channel deforming in simple shear as shown in Fig. 3. A channel of width L in the x direction and infinite extension in the y direction is bounded by walls that are impenetrable for dislocations (i.e., the plastic deformation in the walls is zero). The slip direction corresponds to the x direction, and the layer is sheared by a constant shear stress $\tau_{xy} = \tau_{yx}$. The whole assembly is embedded in an infinite crystal, and it is assumed that the channel, the wall and the embedding crystal have the same elastic constants.

This is a simplified version of a system studied by Van der Giessen and co-workers using both discrete dislocation and continuum plasticity approaches [22]. The simplifications stem from the fact that only a single slip system is assumed to be active, such that reactions between dislocations of different systems need not be considered, and that the boundary conditions reduce to ‘no flux’ conditions for the dislocation fluxes at the bound-

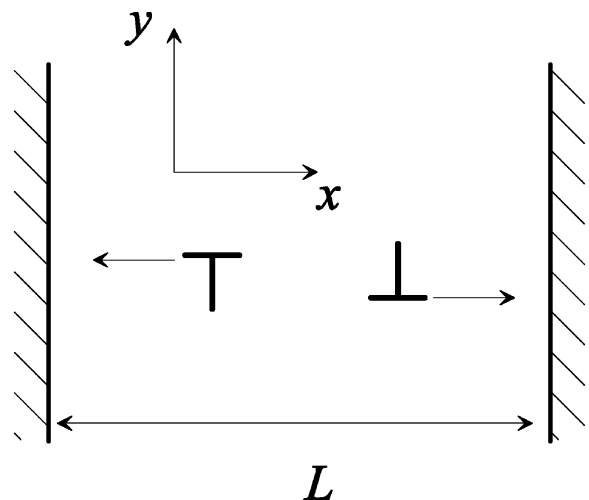


Fig. 3. Geometry of a constrained channel as studied in the text.

ary walls. The system envisaged is particularly simple also because it is homogeneous in the y direction (the dislocation densities depend on the coordinate x in the slip direction only). It follows from Eq. (9) that in this case the long-range self-consistent stress field is zero for an arbitrary function $\kappa(x)$, i.e., any dislocation interactions in the system are of a short-range nature and hence described by the flow stress τ_f and the gradient-dependent stress τ_b .

Before investigating the behavior resulting from Eqs. (26) and (27) and comparing it with the results obtained from discrete simulations, it is instructive to have a look at the results we get from the mean-field model defined by Eqs. (7) and (8). Since the self-consistent stress is zero, the mean-field model becomes trivial: Whatever the initial conditions, for an arbitrarily small positive value of the external stress all positive dislocations ‘condense’ at the right wall and all negative dislocations at the left one. For an initially homogeneous dislocation distribution with density ρ_0 , the strain achieved by this condensation is $\gamma_\infty = \rho_0 b L / 2$. Hence, the system exhibits a trivial size effect (the achievable strain is proportional to the size of the system, which determines the mean dislocation path). However, as demonstrated in the following, the prediction that this strain is achieved at arbitrarily small external stress is grossly unrealistic.

We now revert to the gradient-dependent model derived in the previous section. We assume an initially homogeneous dislocation distribution of density ρ_0 . To facilitate comparison with discrete simulations, it is convenient to introduce scaled stress, space and dislocation density variables through $\tau_{\text{eff}} = Ab\sqrt{\rho_0}\tilde{\tau}$, $x = D\tilde{x}/\sqrt{\rho}$, $\rho = \rho_0\tilde{\rho}$, and $\kappa = \rho_0\tilde{\kappa}$. In scaled variables and after corresponding re-scaling of time, Eqs. (26) and (27) read

$$\partial_t \tilde{\rho}(\tilde{x}, t) = -\partial_{\tilde{x}}[\tilde{\kappa}(\tilde{x}, t) \{ \tilde{\tau} - [1/\tilde{\rho}(\tilde{x}, t)]\partial_{\tilde{x}}\tilde{\kappa}(\tilde{x}, t) \}], \tag{28}$$

$$\partial_t \tilde{\kappa}(\tilde{x}, t) = -\partial_{\tilde{x}}[\tilde{\rho}(\tilde{x}, t) \{ \tilde{\tau} - [1/\tilde{\rho}(\tilde{x}, t)]\partial_{\tilde{x}}\tilde{\kappa}(\tilde{x}, t) \}]. \tag{29}$$

To formulate the boundary conditions at the walls located at $\tilde{x} = \pm \tilde{L}/2$, we note that no dislocations can enter the system through the walls. Hence, the density of positive dislocations (moving to the

right) at the left wall and the density of negative dislocations at the right wall are zero, i.e. $\tilde{\kappa}(-\tilde{L}/2) = -\tilde{\rho}(-\tilde{L}/2)$, $\tilde{\kappa}(\tilde{L}/2) = \tilde{\rho}(\tilde{L}/2)$. Furthermore, the dislocation fluxes at the walls must be zero, which requires that $[\tilde{\rho}\tilde{\tau} - \partial_{\tilde{x}}\tilde{\kappa}] = 0$ at $\tilde{x} = \pm \tilde{L}/2$.

The initial conditions are $\tilde{\rho}(\tilde{x}, 0) = 1$ and $\tilde{\kappa}(\tilde{x}, 0) = 0$ everywhere except directly at the walls where we assume non-zero values of κ , in a narrow boundary layer to satisfy the boundary conditions. We make the simplifying assumption that the effective stress can be represented as the external stress diminished by the (spatially homogeneous) flow stress of an infinite system, and perform a ‘deformation experiment’ as follows: we increase the effective stress from zero in an adiabatically slow manner, i.e., after each small stress increment the system is allowed to relax until it reaches a stationary configuration. After this relaxation, the scaled strain is calculated as $\tilde{\gamma} = -\int \tilde{\kappa} d\tilde{x}$ (cf. Eq. (6)), then the stress is increased again, etc. The resulting stress-strain curves for different values of L are compiled in Fig. 4. It is seen that the behavior is very different from the prediction of the mean-field model: the strain increases gradually with stress and reaches the limit strain γ_∞ ($\tilde{\gamma}_\infty = L/2$ in scaled units) only asymptotically. In physical terms this behavior stems from the fact that there is a short-range repulsion between individual dislocations of the same sign as they pile up against the walls (even though this piling up does not create

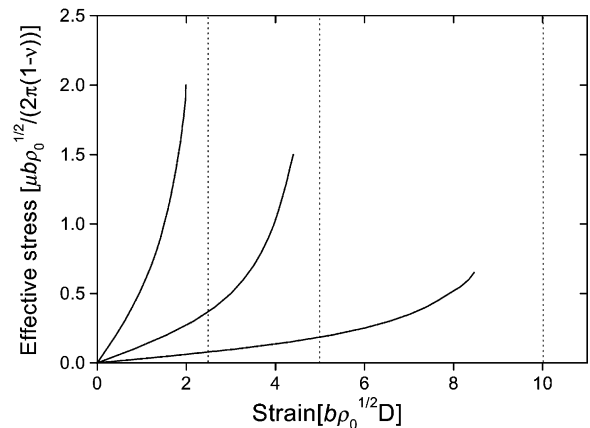


Fig. 4. Stress-strain curves for channels of different width; from left to right: $\tilde{L} = 5, 10, 20$; dotted lines: asymptotic strains λ_∞ for these channel widths.

any long-range stresses!). To increase the strain towards the asymptotic strain, this repulsion must be overcome, which requires an increasing stress that diverges as $\gamma \rightarrow \gamma_\infty$.

Looking at the distribution of dislocation densities and strains within the channel, we find that at high stresses two boundary layers emerge near the walls (Fig. 5). The structure of these boundary layers can be analyzed by noting that at high stresses all dislocations are close to the walls, with only negative dislocations at the left wall ($\bar{\kappa} = -\bar{\rho}$) and only positive dislocations at the right one ($\bar{\kappa} = \bar{\rho}$). In this case Eqs. (28) and (29) reduce, in the stationary case, to

$$\bar{\tau}\bar{\kappa} = \pm \partial_{\bar{x}}\bar{\kappa}, \quad \bar{\kappa} = \bar{\kappa}_0 \tag{30}$$

with the solutions

$$\bar{\kappa}(\bar{x}) = \pm \frac{\bar{\tau}\tilde{L}}{2} \exp[\pm \bar{\tau}(\bar{x} - \{\pm L/2\})] \tag{31}$$

where the + sign applies to the right and the - sign to the left wall. Close to the walls the strain distribution can be written as

$$\tilde{\lambda}(\bar{x}) = \tilde{\gamma}_\infty(1 - \exp[\pm \bar{\tau}(\bar{x} - \{\pm L/2\})]). \tag{32}$$

We see that there is an exponential increase of the dislocation density towards and an exponential increase of the strain from the walls. The width of the boundary layer within which this increase takes

place is $1/\bar{\tau}$, or $\Delta x = ADb/\tau_{eff}$ dimensional units, i.e., it is inversely proportional to the stress that ‘presses’ the dislocations against the wall. Interestingly, the width of the boundary layer depends only on the effective stress, but not on the channel width or the dislocation density.

To verify the predictions of the continuum model, discrete simulations have been carried out. Since we are interested only in the quasi-static behavior of the dislocation system, an automaton model has been used where dislocations move on a lattice depending on the sign of the local stresses acting on them (these are given by the expression in the parentheses on the right-hand side of Eq. (1)). The lattice constant Δ which defines the elementary length of the simulation has been chosen sufficiently small such that a variation of Δ by a factor of 2 did not significantly affect the results. To mimic the infinite extension of the system, periodic boundary conditions have been imposed in the y direction. Simulations have been carried out at different system sizes and dislocation densities. In each case, equal numbers of dislocations of both signs were initially distributed at random over a system of length L such that the dislocation density was ρ_0 . Then the dislocation arrangement was allowed to relax at zero stress, and subsequently a ‘deformation test’ was carried out by incrementally increasing the external stress, allowing the dislocation arrangement to relax until all dislocations have come to rest, further increasing the stress, etc. In each step the total strain was computed from the sum of the dislocation paths. To allow comparison with the continuum model, the effective stresses have been determined by subtracting from the external stresses the flow stress of an infinite system (determined from a system that is periodic in the x direction with a large periodicity length, for the method used in determining the flow stress, see [20]).

To obtain reliable statistics, stress-strain graphs and the corresponding dislocation density profiles were averaged over a huge ensemble (typically several thousands of simulations). An example of a dislocation density profile obtained from this procedure is illustrated in Fig. 5 which shows a $\bar{\kappa}(\bar{x})$ profile averaged over 2000 simulations of systems with length $L = 4/\sqrt{\rho_0}$ and (periodically repeated)

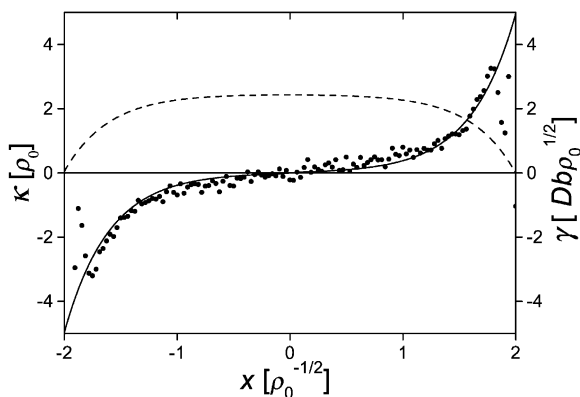


Fig. 5. Sign dislocation density and strain profiles for a system of width $L = 4/\sqrt{\rho_0}$ at scaled stress $\bar{\tau} = 2$; Data points: $\kappa(x)$ from discrete simulation; full line: $\kappa(x)$ from continuum model with $D = 0.8$; dashed line: strain profile from continuum model.

height $16/\sqrt{\rho_0}$. The profile shown in the figure has been taken at a scaled effective stress $\bar{\tau} = 2$. It is seen that indeed two boundary layers emerge. From the width of these boundary layers we can directly determine the constant D for the present type of simulation, which turns out to be $D = 0.8$. Using the continuum model with this value of D yields the full line in Fig. 5, which shows that the density profile obtained from the continuum model matches well the discrete simulation except in the immediate vicinity of the walls. As seen from Fig. 6, also the stress-strain curves for the discrete and continuum models exhibit almost perfect agreement. By varying the system size and initial dislocation density, we find that for sufficiently high stresses the width of the boundary layers at fixed stress τ_{ext} is within the error margins indeed independent on the system size and the dislocation density. If the applied stress is increased, the boundary layer width is found to decrease. Again all these findings are in line with the predictions of the continuum model.

5. Conclusions

We have obtained a continuum model of dislocation dynamics from statistically averaging the equations of motion of discrete dislocations. In this

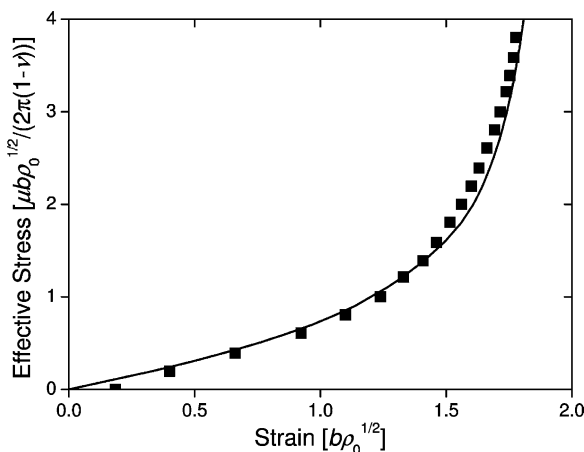


Fig. 6. Comparison of stress-strain graphs; full line: continuum model; data points: discrete simulation. Parameters are the same as in Fig. 5, for these parameters $\gamma_c \sqrt{\rho_0}$.

model the dislocation fluxes are governed by different stress contributions, viz., the external stress, a long-range stress created by ‘geometrically necessary’ excess dislocations related to strain gradients, and a stress contribution which characterizes short-range interactions between individual dislocations. Mathematically this stress contribution is related to the presence of non-vanishing short-range correlations in the dislocation arrangement. It can be approximated as a sum of two contributions, namely a local flow stress which scales as the square root of the dislocation density, and a gradient-dependent term. Because of this term the dislocation dynamics equations have the structure of generalized diffusion equations. It can alternatively be interpreted as a second-order strain gradient contribution to the flow stress as envisaged by Aifantis [21], with an internal length scale that is proportional to the dislocation spacing.

Comparing the predictions of the continuum model with the results of discrete simulations for a very simple system demonstrates that this model captures essential properties of dislocation-dislocation interactions in a continuum framework. We have considered a very simple situation (single slip, conserved dislocation number) to demonstrate the method, but our approach can be straightforwardly extended to general 2D dislocation systems in which dislocation reactions and/or dislocation multiplication may occur, and where several slip systems may be active. For such systems, the present approach offers a systematic procedure for resolving issues related to the link between discrete dislocation dynamics and continuum plasticity as discussed in [18,22]. The generalization of the approach to three dimensions where dislocations have to be treated as flexible lines remains, however, a substantial challenge.

Acknowledgements

The authors are grateful to Professor E. Aifantis for valuable discussions. The financial support of the Hungarian Scientific Research Fund (OTKA) under contract number T 030791 and of the European Commission under contract No. ERB FMRX-CT96-0062 is gratefully acknowledged.

Appendix A Correlation functions and gradient terms

The combinations of two-particle density functions appearing in Eqs. (4, 5) have the form:

$$\begin{aligned} & \rho_{++}(\vec{r}_1, \vec{r}_2) - \rho_{--}(\vec{r}_1, \vec{r}_2) - \rho_{+-}(\vec{r}_1, \vec{r}_2) \\ & + \rho_{-+}(\vec{r}_1, \vec{r}_2) = \frac{1}{4} \{ \rho(\vec{r}_1) \rho(\vec{r}_2) [d_{++}(\vec{r}_{12}) \\ & - d_{--}(\vec{r}_{12}) + d_{+-}(\vec{r}_{12}) - d_{-+}(\vec{r}_{12})] \\ & + \kappa(\vec{r}_1) \kappa(\vec{r}_2) [4 + d_{++}(\vec{r}_{12}) + d_{--}(\vec{r}_{12}) \\ & + d_{+-}(\vec{r}_{12}) + d_{-+}(\vec{r}_{12})] \\ & + \rho(\vec{r}_1) \kappa(\vec{r}_2) [d_{++}(\vec{r}_{12}) - d_{--}(\vec{r}_{12}) - d_{+-}(\vec{r}_{12}) \\ & - d_{-+}(\vec{r}_{12})] \} + \kappa(\vec{r}_1) \rho(\vec{r}_2) [d_{++}(\vec{r}_{12}) \\ & - d_{--}(\vec{r}_{12}) - d_{+-}(\vec{r}_{12}) - d_{-+}(\vec{r}_{12})] \} \end{aligned} \quad (33)$$

$$\begin{aligned} & \rho_{++}(\vec{r}_1, \vec{r}_2) - \rho_{--}(\vec{r}_1, \vec{r}_2) - \rho_{+-}(\vec{r}_1, \vec{r}_2) \\ & + \rho_{-+}(\vec{r}_1, \vec{r}_2) = \frac{1}{4} \{ \rho(\vec{r}_1) \rho(\vec{r}_2) [d_{++}(\vec{r}_{12}) \\ & - d_{--}(\vec{r}_{12}) + d_{+-}(\vec{r}_{12}) - d_{-+}(\vec{r}_{12})] \\ & + \kappa(\vec{r}_1) \kappa(\vec{r}_2) [d_{++}(\vec{r}_{12}) - d_{--}(\vec{r}_{12}) \\ & + d_{+-}(\vec{r}_{12}) + d_{-+}(\vec{r}_{12})] + \rho(\vec{r}_1) \kappa(\vec{r}_2) [4 \\ & + d_{++}(\vec{r}_{12}) + d_{--}(\vec{r}_{12}) + d_{+-}(\vec{r}_{12}) \\ & + d_{-+}(\vec{r}_{12})] + \kappa(\vec{r}_1) \rho(\vec{r}_2) [d_{++}(\vec{r}_{12}) \\ & + d_{--}(\vec{r}_{12}) - d_{+-}(\vec{r}_{12}) - d_{-+}(\vec{r}_{12})] \} \end{aligned} \quad (34)$$

Taking into account that in a quasi-homogeneous system $d_{++}(\vec{r}) = d_{--}(\vec{r})$ and $d_{+-}(\vec{r}) = d_{-+}(-\vec{r})$, and introducing the notations $d^p(\vec{r}) = d_{++}(\vec{r})$, $d^s(\vec{r}) = (d_{+-}(\vec{r}) + d_{-+}(-\vec{r}))/2$, and $d^a(\vec{r}) = (d_{+-}(\vec{r}) - d_{-+}(-\vec{r}))/2$, expressions (33, 34) simplify to

$$\begin{aligned} & \rho_{++}(\vec{r}_1, \vec{r}_2) + \rho_{--}(\vec{r}_1, \vec{r}_2) - \rho_{+-}(\vec{r}_1, \vec{r}_2) \\ & - \rho_{-+}(\vec{r}_1, \vec{r}_2) = \frac{1}{2} \{ \rho(\vec{r}_1) \rho(\vec{r}_2) [d^p(\vec{r}_{12}) \\ & - d^s(\vec{r}_{12})] + \kappa(\vec{r}_1) \kappa(\vec{r}_2) [2 + d^p(\vec{r}_{12}) \\ & + d^s(\vec{r}_{12})] + \rho(\vec{r}_1) \kappa(\vec{r}_2) d^a(\vec{r}_{12}) \\ & - \kappa(\vec{r}_1) \rho(\vec{r}_2) d^a(\vec{r}_{12}) \}, \end{aligned} \quad (35)$$

$$\begin{aligned} & \rho_{++}(\vec{r}_1, \vec{r}_2) - \rho_{--}(\vec{r}_1, \vec{r}_2) - \rho_{+-}(\vec{r}_1, \vec{r}_2) \\ & + \rho_{-+}(\vec{r}_1, \vec{r}_2) = \frac{1}{2} \{ -\rho(\vec{r}_1) \rho(\vec{r}_2) d^a(\vec{r}_{12}) \\ & + \kappa(\vec{r}_1) \kappa(\vec{r}_2) d^a(\vec{r}_{12}) + \rho(\vec{r}_1) \kappa(\vec{r}_2) [2 \\ & + d^p(\vec{r}_{12}) + d^s(\vec{r}_{12})] + \kappa(\vec{r}_1) \rho(\vec{r}_2) [d^p(\vec{r}_{12}) \\ & - d^s(\vec{r}_{12})] \}. \end{aligned} \quad (36)$$

With these notations Eqs. (4, 5) become

$$\begin{aligned} & \frac{\partial \rho(\vec{r}, t)}{\partial t} + \frac{\partial}{\partial \vec{r}} \vec{b} [\kappa(\vec{r}, t) \{ \tau_{sc}(\vec{r}) + \tau_{ext} - \tau_f(\vec{r}) \\ & + \tau_b(\vec{r}) \} + \rho(\vec{r}, t) \tau_a(\vec{r})] = 0, \end{aligned} \quad (37)$$

$$\begin{aligned} & \frac{\partial \kappa(\vec{r}, t)}{\partial t} + \frac{\partial}{\partial \vec{r}} \vec{b} [\rho(\vec{r}, t) \{ \tau_{sc}(\vec{r}) + \tau_{ext} - \tau_f(\vec{r}) \\ & + \tau_b(\vec{r}) \} + \kappa(\vec{r}, t) \tau_a(\vec{r})] = 0, \end{aligned} \quad (38)$$

where

$$\tau_b(\vec{r}) = \frac{1}{2} \int [\kappa(\vec{r}_1) (d^p(\vec{r} - \vec{r}_1) + d^s(\vec{r} - \vec{r}_1))] \quad (39)$$

$$\tau_f(\vec{r}) = \rho(\vec{r}_1) d^a(\vec{r} - \vec{r}_1) \tau_{ind}(\vec{r} - \vec{r}_1) d\vec{r}_1, \quad (40)$$

$$\begin{aligned} \tau_a(\vec{r}) = \frac{1}{2} \int & [\rho(\vec{r}_1) (d^p(\vec{r} - \vec{r}_1) - d^s(\vec{r} - \vec{r}_1)) \\ & + \kappa(\vec{r}_1) d^a(\vec{r} - \vec{r}_1)] \tau_{ind}(\vec{r} - \vec{r}_1) d\vec{r}_1, \end{aligned} \quad (41)$$

and the self-consistent stress τ_{sc} is defined by Eq. (9). To further simplify these equations we revert to the evolution equations of the densities of positive and negative dislocations and note that these equations can be envisaged as continuity equations. By adding and subtracting Eqs. (37) and (38) we find

$$\begin{aligned} & \frac{\partial \rho_+(\vec{r}, t)}{\partial t} = \frac{\partial}{\partial \vec{r}} \vec{b} [\rho_+(\vec{r}, t) \{ \tau_{sc} + \tau_{ext} - \tau_f + \tau_b \\ & + \tau_a \}] = \frac{\partial}{\partial \vec{r}} [\rho_+(\vec{r}, t) \vec{v}_+(\vec{r}, t)] \end{aligned} \quad (42)$$

$$\frac{\partial \rho_{-}(\vec{r}, t)}{\partial t} = \frac{\partial}{\partial \vec{r}} \vec{b} [\rho_{-}(\vec{r}, t) \{ \tau_{sc} + \tau_{ext} - \tau_f + \tau_b + \tau_a \}] = - \frac{\partial}{\partial \vec{r}} [\rho_{-}(\vec{r}, t) \vec{v}_{-}(\vec{r}, t)]. \quad (43)$$

Since dislocations of opposite signs move at each given point with equal velocities but in opposite directions, $\vec{v}_{+}(\vec{r}) = -\vec{v}_{-}(\vec{r})$. It follows from Eqs. (42, 43) that $\tau_a = 0$. Hence, the effect of dislocation pair correlations is completely contained in the ‘flow stress’ τ_f and the ‘back stress’ τ_b .

References

- [1] Holt DL. Journal App1 Phys 1970;41:3179.
- [2] Rickman JM, Vifials J. Phil Mag A 1997;75:1251.
- [3] Walgraef D, Aifantis EC. J App1 Phys 1985;15:688.
- [4] Walgraef D, Aifantis EC. Int J Eng Sci 1985;23:1359.
- [5] Walgraef D, Aifantis EC. Int J Eng Sci 1985;23:1365.
- [6] Franek A, Kalus R, Kratochvil J. Phil Mag A 1991;64:497.
- [7] Kratochvil J, Saxlova M. Scripta Met Mater 1993;26:113.
- [8] Hdhner P. Acta Mater 1996;44:2345.
- [9] Hdhner P, Bay K, Zaiser M. Phys Rev Lett 1998;81:2470.
- [10] Groma I. Phys Rev B 1997;56:5807.
- [11] Groma I, Balogh P. Acta Mater 1999;.
- [12] E1-Azab A. Phys Rev B 2000;61:11956.
- [13] Zaiser M, Miguel M-C, Groma I. Phys Rev 2001;64:224102.
- [14] Landau, L.D., Lifshitz, E.M., In theory of elasticity, course in theoretical physics Vol. 7. 3rd ed. Oxford:Pergamon, 86.
- [15] Wilkens M. Acta Metall 1967;15:1412.
- [16] Groma I, Bakó B. Phys Rev B 1998;58:2964.
- [17] Groma I. Phys Rev B 1998;57:7535.
- [18] Yefimov S, Groma I, Van der Giessen EJ. Phys IV France 2001;11:103.
- [19] Zaiser M, Aifantis EC. Scripta Mater 2002 in press.
- [20] Miguel, M.C., Vespignani, A., Zaiser, M., Zapperi, S., Phys Rev Lett 2002, submitted.
- [21] Aifantis EC. Int J Plasticity 1987;3:211.
- [22] Cleveringa HHM, Van der Giessen E, Needleman A. Acta Mat 1997;54:3164.